Rock-scissors-paper game on regular small-world networks

2004 J. Phys. A: Math. Gen. 37 2599

(http://iopscience.iop.org/0305-4470/37/7/006)

INSTITUTE OF PHYSICS PUBLISHING JOURNAL OF PHYSICS A: MATHEMATICAL AND GENERAL

J. Phys. A: Math. Gen. **37** (2004) 2599–2609 PII: S0305-4470(04)64841-4

Rock-scissors-paper game on regular small-world networks

György Szabó[1], **Attila Szolnoki**[1] **and Rudolf Izsák**[2]

[1] Research Institute for Technical Physics and Materials Science, PO Box 49, H-1525 Budapest, Hungary
[2] Institute for Theoretical Physics, Eötvös University, PO Box 32, H-1518 Budapest, Hungary

Received 16 June 2003, in final form 16 December 2003
Published 4 February 2004
Online at stacks.iop.org/JPhysA/37/2599 (DOI: 10.1088/0305-4470/37/7/006)

Abstract

The spatial rock-scissors-paper game (or cyclic Lotka–Volterra system) is extended to study how the spatiotemporal patterns are affected by the rewired host lattice providing uniform number of neighbours (degree) at each site. On the square lattice this system exhibits a self-organizing pattern with equal concentration of the competing strategies (species). If the quenched background is constructed by substituting random links for the nearest-neighbour bonds of a square lattice then a limit cycle occurs when the portion of random links exceeds a threshold value. This transition can also be observed if the standard link is replaced temporarily by a random one with a probability P at each step of iteration. Above a second threshold value of P the amplitude of global oscillation increases with time and finally the system reaches one of the homogeneous (absorbing) states. In this case the results of Monte Carlo simulations are compared with the predictions of the dynamical cluster technique evaluating all the configuration probabilities on one-, two-, four- and six-site clusters.

PACS numbers: 05.50.+q, 89.75.Hc

1. Introduction

The rock-scissors-paper like cyclic dominance among three states (modes, species, strategies, opinions) is widely studied in different spatial systems. For example, the Rayleigh–Bernard convection in fluid layers rotating around a vertical axis exhibits the Küpper–Lortz instability [1] resulting in a cyclic change of the three possible directions of parallel convection rolls [2–4]. Such a situation can appear in biological (ecological) systems too [5–8]. Very recently, Kerr *et al* [9] have justified experimentally that the cyclic dominance between the toxic, sensitive and resistant microbes maintains their coexistence as predicted previously by several theoretical works [10–12]. The emergence of cyclic invasions has also been observed for

some three-strategy evolutionary games where this phenomenon promotes cooperation among selfish individuals [13–15].

The above three-state systems exhibit some general features. Namely, spiral formation (or rotating three-edge vortices and antivortices) can occur on the two-dimensional backgrounds [16–18] as is observed for the Belousov–Zhabotinskii reaction as well as for the numerical investigation of excitable activator–inhibitor media [19]. This self-organizing structure can provide stability against some external invaders and thereby it plays a crucial role in ecological systems [20, 21]. Furthermore the cyclic dominance yields a paradoxical response to the external support of one of the species [22, 23] and global oscillation can occur when varying either the model [24] or the structural parameters [25] if long range interactions are allowed.

In this work the spatial rock-scissors-paper game will be extended for such regular networks where each site has four neighbours. We discuss how the quenched randomness and annealed randomness of the network affect the spatiotemporal distribution of species. Such a comparison has already been performed for a rumour propagation model [26, 27]. Now, the randomness is introduced in a small-world manner [28] leaving the degree of sites unchanged. This restriction does not influence the small-world feature of the network and it simplifies the application of some theoretical approximation at least for the case of annealed randomness. However, the main conclusion remains valid for both types of randomness. The Monte Carlo (MC) simulations indicate that these systems undergo a transition (Hopf bifurcation) from a stationary state (with fixed average concentrations) to a global oscillation. The amplitude of oscillation increases with the measure of randomness and the increasing oscillation terminates at one of the absorbing (homogeneous) states above a second threshold value for annealed randomness. We show that neither the mean-field nor the pair approximations can explain these transitions. The failure of these descriptions has inspired us to use the more sophisticated dynamical cluster techniques where one determines all the configuration probabilities on a k-site cluster. At the levels of $k = 1$ and 2 this technique is equivalent to the mentioned mean-field and pair approximations. The essence of this simple method is described in [29, 30].

2. The model

We consider a very simple model where the sites of a regular graph are occupied by one of the three species ($s_i = 1, 2, 3$) that dominate cyclically each other. The evolutionary process is governed by the sequence of elementary invasions along the randomly chosen edges of the graph. Namely, first we choose a site and one of its linked (neighbouring) sites at random. If these two sites are occupied by different species then the predator occupies the prey's site, i.e., the (1, 2) and (2, 1) pairs transform into (1, 1), (2, 3) and (3, 2) into (2, 2), and (1, 3) and (3, 1) into (3, 3). Starting from a random initial state the above process is repeated until the system reaches the stationary state or the limit cycle we study. This system was already analysed systematically by several authors for the case when the sites form a d-dimensional lattice [17, 31].

Two types of random structures will be contrasted with each other. In the first case the structure is quenched after the generation of edges. Figure 1 illustrates an example whose creation is similar to those suggested by Watts and Strogatz [28]. Note, that the present algorithm (explained in the caption of figure 1) conserves the degree of sites, i.e., the number of neighbours remains fixed ($z = 4$) for each site. In the second case the 'neighbourhood' is not fixed in time, that is a randomly chosen new site can be replaced for any standard neighbours during the elementary invasions explained above. These types of random networks can characterize the interaction among individuals in social systems [24, 28, 32–34]. In both

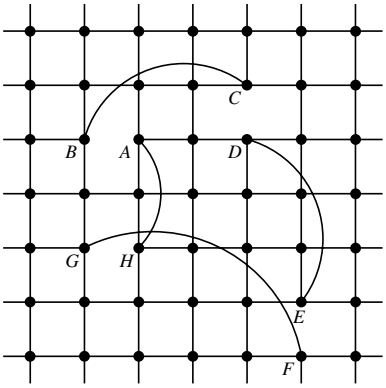

Figure 1. Structure of a regular small-world network whose construction starts from a square lattice. First the randomly chosen AB link is removed and the site B is rewired to the randomly chosen site C. To have four connections at site C we eliminate one of the previous links (here CD) and add a new link DE at random. This process is repeated till Q portion of the nearest-neighbour bonds is replaced by random links. Finally the last site (here H) is wired to the first one (A). The edges pointing out along the periphery refer to periodic boundary conditions assumed for the original square lattice.

cases the random links connect two sites that are at an arbitrary distance from each other in the original structure.

The measure of quenched randomness is characterized by the Q portion of random links substituted for the nearest-neighbour bonds. If $Q = 0$ this structure reproduces the square lattice and for $Q = 1$ it is equivalent to a random regular graph [35] where the typical local structure is analogous to a Cayley tree for large number of sites N. Previous investigations indicated that some phenomena on the random regular graphs can be well described analytically if the background is assumed to be a Bethe lattice in the limit $N \to \infty$ [24, 36]. In other words, the structure with $Q = 1$ can be considered as a possible realization of the Bethe lattice in the simulations for large N.

Unfortunately, the present random regular structures with $0 < Q < 1$ are not yet investigated rigorously, although many other classes of networks are well studied [37–40]. We think that the constraint of regularity leaves the relevant features unchanged and the present structure remains similar to those introduced by Watts and Strogatz [28] on a square lattice. When increasing Q the present structure exhibits a continuous transition from the square lattice to the random regular graph.

Besides the above quenched randomness we will investigate the consequences of the annealed (temporal) randomness in the structure. In this case the standard links are defined by the bonds between the nearest-neighbour sites forming a square lattice. Occasionally the standard link is replaced by a random one with a probability P characterizing the strength of annealed randomness. Evidently, for $P = 0$ the structure is equivalent to the square lattice. On the other hand, in the limit $P \to 1$ this system satisfies the conditions of mean-field approaches.

3. Simulations

The MC simulations are performed on a network consisting of $N = L \times L$ sites where the linear size of the square lattice (L) is varied from 400 to 3200. The regular small-world networks are constructed from a square lattice repeating the rewiring steps $-2N \ln(1 - Q)$

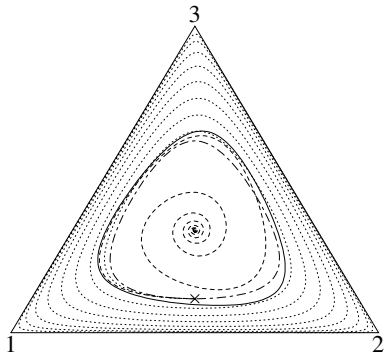

Figure 2. The MC simulations show four typical trajectories plotted on the ternary phase diagram. All the simulations are started from the same initial state (denoted by symbol X) on the square lattice for $L = 3200$. If $P = 0$ then the system develops into the central fixed point (dashed line). For $P = 0.2$ the growing spiral trajectory (dotted line) ends at one of the homogeneous states. The solid line indicates only the limit cycle towards the growing (or shrinking) spiral trajectories that evolve for $P = 0.05$. In the mean-field limit ($P = 1$) the trajectory (dashed-dotted line) returns periodically to the initial state.

times as explained in the caption of figure 1. (The logarithmic correction takes into account that the substitution of a random link for another random one does not increase the quenched randomness.)

The above model has two parameters characteristic of the quenched (Q) and annealed (P) randomness of the background. The present analysis is restricted to those cases when one of them is chosen to be zero.

For small sizes ($L < 10$) this system evolves into one of the three absorbing states where all the sites are occupied by the same species. For sufficiently large system sizes, however, the three species can coexist and after some transient time the state can be well described by the current concentration of the three species [$c_1(t) + c_2(t) + c_3(t) = 1$]. In order to observe these states we have to choose such a large L where the amplitude of fluctuations becomes significantly less than the minimum value of concentrations. The above choices satisfy this condition.

On the square lattice ($Q = P = 0$) this system develops into a stationary state where all three species are present with the same average concentration, i.e., $\langle c_1 \rangle = \langle c_2 \rangle = \langle c_3 \rangle = 1/3$ corresponding to the central point in the ternary phase diagram as plotted in figure 2. In this case the three species alternate cyclically at each site and the short range interactions are not able to synchronize these local oscillations.

The corresponding self-organizing spatiotemporal patterns are well investigated previously by several authors [17, 31, 41]. In these patterns the rotating vortices (spirals) and antivortices are not recognizable because of the interfacial roughening. The absence of smooth interfaces (surface tension) is caused by the fact that the elementary invasions between two neighbouring sites are not affected by their neighbourhood [18].

Global oscillation (synchronization) occurs when the frequency of random (long range) links exceeds a threshold value depending on whether quenched or annealed randomness is considered. To illustrate the time-dependence of the species distributions during a period of this global oscillation six consecutive snapshots are plotted in figure 3.

The amplitude of oscillation increases with the measure of randomness in both cases. If the annealed randomness exceeds a second threshold value then the trajectories approach the edges of the triangle and sooner or later the evolution is terminated at one of the homogeneous

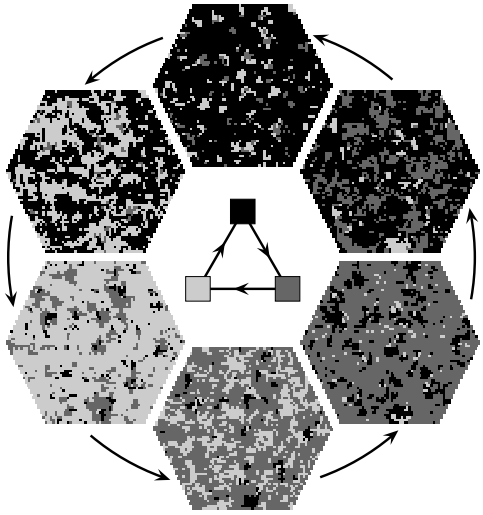

Figure 3. The hexagonal snapshots represent consecutive species distributions on a small portion of square lattice during the MC simulation of global oscillation for $Q = 0$ and $P = 0.1$. Arrows along the periphery indicate the direction of time evolution. The cyclic food web is shown in the centre where the three species are denoted by different grey scales as in the snapshots and the arrows point to the direction of invasion between the species. Thus, the territory of the 'black' species will be occupied by the 'light-grey' species. Once the 'light-grey' species prevail, they will be invaded by the 'dark-grey' species, and finally a 'black' invasion closes the cycle as shown by the snapshots.

(absorbing) states (where the system stays forever). It is emphasized, however, that the homogeneous states are not stable against the invasion of their predators. For example, the offsprings of a single species 3 will occupy the whole territory of species 1 in the absence of species 2.

In the ternary phase diagram the shape of the limit cycles reflects the cyclic symmetry between the species and its extension is described by the area A compared to its maximum value. The average value of this quantity can be easily determined by numerical integration after a suitable relaxation time for either the MC simulations or the dynamical cluster techniques. Evidently, A vanishes if the system tends towards the central fixed point, and it goes to 1 when the trajectories approach the edges of the triangle (see figure 2).

Systematic MC simulations are carried out to determine the average value of A on the regular small-world structure for different Q values. The results in figure 4 refer to a transition from a fixed point to the limit cycle. For weak randomness ($Q < Q_1 = 0.067(1)$) the system always tends to the central fixed point. Conversely, oscillating behaviour occurs and the area A (as well as the amplitude) of the limit cycle increases monotonically with Q and tends to the value $A(Q = 1) = 0.980(1)$. The limit $Q \to 1$ is investigated on a random regular graph created by using a different algorithm [36]. In the vicinity of the transition point A vanishes linearly with $Q - Q_1$ in agreement with the prediction of Hopf bifurcation describing the emergence of a limit cycle in a mean-field type system if the model parameters are varied. Further rigorous investigations are required to quantify the variations in the spatiotemporal patterns when approaching the transition point.

As is already mentioned the system size should be large enough to avoid the finite size effects. The sharp transition to the global oscillation is wiped out by fluctuations on smaller systems as discussed previously by Kuperman and Abramson [25] who considered a

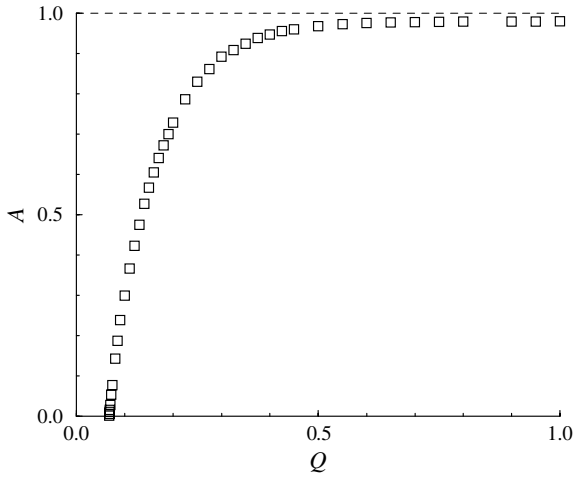

Figure 4. Relative area of limit cycle versus Q for a regular small-world system sketched in figure 1.

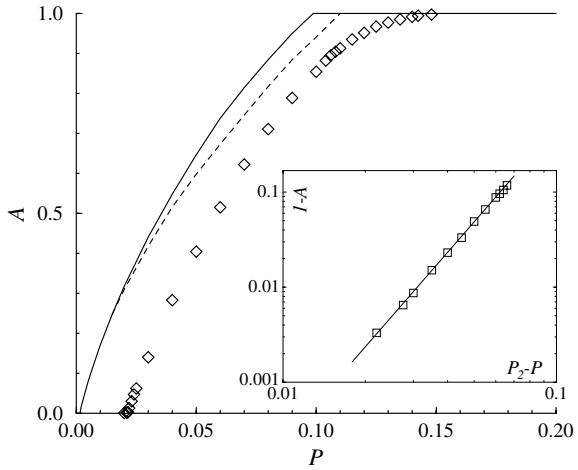

Figure 5. Relative area of the limit cycle as a function of P characteristic of the annealed randomness. The symbols indicate the MC data, the solid and dashed lines illustrate the prediction of four- and six-site dynamical cluster techniques. The inset shows the log–log plot of $1 - A$ versus $P_2 - P$.

three-state (cyclic) epidemiological model on small-world networks suggested by Watts and Strogatz [28]. The finite size effects are more dangerous when the value of area A approaches 1. In this case the evolution may be easily trapped by one of the absorbing states. This difficulty is avoided by choosing a sufficiently large system size. As a result, the plotted $A(Q)$ function may be considered as the infinite size limit.

The above analysis was repeated for the annealed randomness when varying P for $Q = 0$. The results of MC simulations are summarized in figure 5. The oscillating behaviour can be observed for $P_1 < P < P_2$ where $P_1 = 0.020(1)$ and $P_2 = 0.170(1)$. If $P > P_2$ then the increasing spiral trajectory terminates in one of the absorbing states as demonstrated in figure 2. In the vicinity of the first threshold value $A \propto (P - P_1)$ in agreement with the expectation.

In contrast, A approaches 1 very smoothly when P goes to P_2. Surprisingly, our MC data can be well approximated by a power law behaviour ($1 - A \propto (P_2 - P)^{\gamma}$) as indicated in the inset of figure 5. The numerical fit yields $\gamma = 3.3(3)$.

It is worth mentioning that the emergence of global oscillation has already been observed in the above-mentioned epidemiological model when varying the quenched randomness without the constraints of regularity [25]. The similar behaviour refers to the robustness of this type of transition.

4. Extended mean-field analysis

The predictions of the traditional mean-field analysis are well discussed in the textbook by Hofbauer and Sigmund [42]. According to this approach four stationary states exist, namely, the above-mentioned three absorbing states (e.g. $c_1 = 1$ and $c_2 = c_3 = 0$) and the well-mixed symmetric state where the three species are present with the same concentration (1/3). Besides these stationary solutions the mean-field analysis shows the existence of a set of oscillating states whose closed trajectories draw concentric orbits around the centrum in the ternary phase diagram. Along these orbits the product $c_1c_2c_3$ is conserved. In agreement with the expectation the MC simulations reproduce this behaviour for $P = 1$ as shown in figure 2.

The application of the pair approximation is inspired by its success when investigating an evolutionary game with three (cyclically dominated) strategies on a random regular graph [24]. This model exhibits both transitions mentioned above when varying the parameter(s) of the payoff matrix. It is underlined that here the adoption of the neighbouring strategies depends on the neighbourhood.

In the pair approximations one determines the $p_2(s_1, s_2)$ probability of finding the (s_1, s_2) configuration on two nearest-neighbour (or linked) sites. In this case equations of motion are derived for these quantities taking into account the contribution of all the elementary invasion processes (details are given in the textbook by Marro and Dickman [29]). The numerical integration of the corresponding equations predicts growing spirals approaching the boundaries (and resulting in the maximum value $A = 1$ in the limit $t \to \infty$) as indicated in figure 2. This prediction is in contrast to the results of MC simulations obtained on either the square lattice ($A = 0$) or the random regular graphs ($A = 0.98$). We have to emphasize that although the equations of motion involve explicitly the number of neighbours the simple pair approximation cannot distinguish the structure of the Bethe and square lattices. In the light of previous experiences [24] it is expected that the pair approximation can well describe the behaviour observed by MC simulations on the random regular graph because in this structure the average loop size increases with $\ln N$ [35]. Thus, for large N, the local structure is tree-like and the short range correlations between two sites can be well approximated by a product of the $p_2(s, s')$ configuration probabilities involved along the single path connecting the two sites. The comparison of the above values of A does not confirm this expectation. More precisely, the pair approximation cannot account for the effect preventing the unlimited growth of the area of the limit cycle. Preliminary results suggest that the limit value of A depends on the degree of the random regular graph. In the near future we wish to study this effect by a suitable extension of the dynamical cluster techniques. Henceforth, however, our efforts will be concentrated on the annealed randomness because its investigation can be easily built into the dynamical cluster technique. At the level of pair approximation the corresponding results predict that the 'spiral pitch' decreases when P is increased and vanishes in the mean-field limit ($P = 1$) as expected.

On the square lattice, as mentioned above, the pair approximation is not capable of describing the appearance of self-organizing patterns maintained by the interfacial motions

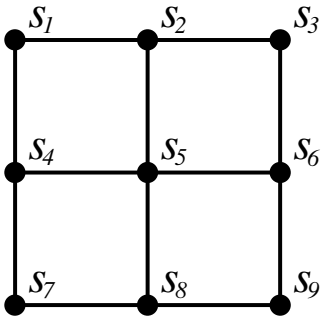

Figure 6. The invasion of the central site from its neighbouring sites affects all the four four-site configuration probabilities.

due to cyclic invasions. This striking shortage can be eliminated by choosing larger and larger clusters on which we determine all the possible configuration probabilities [29]. For example, at the level of four-site approximation we determine the configuration probabilities $p_4(s_1, s_2, s_3, s_4)$ on a 2×2 cluster assumed to be translation invariant on the square lattice. A recent summary of larger-cluster approximations can be found in [30].

This approach takes explicitly into account some topological features of the square lattice. A nearest-neighbour invasion (e.g. $s_4 \to s_5$ as demonstrated in figure 6) will simultaneously affect all the four four-site configuration probabilities involved. The spatial effect is taken into account more rigorously if the probability of such a nine-site constellation is approximated as

$$p_9(s_1, \ldots, s_9) = \frac{p_4(s_1, s_2, s_4, s_5)\, p_4(s_2, s_3, s_5, s_6)}{p_2(s_2, s_5)\, p_2(s_4, s_5)} \times \frac{p_4(s_4, s_5, s_7, s_8)\, p_4(s_5, s_6, s_8, s_9)}{p_2(s_5, s_6)\, p_2(s_5, s_8)}\, p_1(s_5) \tag{1}$$

where the configuration probabilities satisfy the following compatibility conditions:

$$\begin{aligned} p_1(s_1) &= \sum_{s_2} p_2(s_1, s_2) = \sum_{s_2} p_2(s_2, s_1) \\ p_2(s_1, s_2) &= \sum_{s_3, s_4} p_4(s_1, s_2, s_3, s_4) = \sum_{s_3, s_4} p_4(s_3, s_4, s_1, s_2) \\ &= \sum_{s_3, s_4} p_4(s_1, s_3, s_2, s_4) = \sum_{s_3, s_4} p_4(s_3, s_1, s_4, s_2). \end{aligned} \tag{2}$$

The time derivative of $p_4(s_1, s_2, s_3, s_4)$ can be described by a master equation that summarizes the contribution of all the possible elementary invasions. Namely,

$$\begin{aligned} \frac{\mathrm{d}}{\mathrm{d}t} p_4(s_1, s_2, s_3, s_4) &= -P \sum_{s_x} p_4(s_1, s_2, s_3, s_4)\, p_1(s_x)[\Gamma(s_x, s_1) + \Gamma(s_x, s_2) + \Gamma(s_x, s_3) + \Gamma(s_x, s_4)] \\ &+ P \sum_{s_x} p_4(s_x, s_2, s_3, s_4)\, p_1(s_1)\Gamma(s_1, s_x) \\ &+ P \sum_{s_x} p_4(s_1, s_x, s_3, s_4)\, p_1(s_2)\Gamma(s_2, s_x) \\ &+ P \sum_{s_x} p_4(s_1, s_2, s_x, s_4)\, p_1(s_3)\Gamma(s_3, s_x) \end{aligned}$$

$$
\begin{aligned}
&+ P \sum_{s_x} p_4(s_1, s_2, s_3, s_x)\, p_1(s_4)\Gamma(s_4, s_x) \\
&- \frac{1-P}{4} \sum_{s_5,s_6,s_7,s_8,s_9} p_9(s_1, s_2, s_5, s_3, s_4, s_6, s_7, s_8, s_9)\Gamma(s_2, s_4) \\
&- \frac{1-P}{4} \sum_{s_5,s_6,s_7,s_8,s_9} p_9(s_5, s_1, s_2, s_6, s_3, s_4, s_7, s_8, s_9)\Gamma(s_1, s_3) \\
&- \frac{1-P}{4} \sum_{s_5,s_6,s_7,s_8,s_9} p_9(s_5, s_6, s_7, s_1, s_2, s_8, s_3, s_4, s_9)\Gamma(s_6, s_2) \\
&- \frac{1-P}{4} \sum_{s_5,s_6,s_7,s_8,s_9} p_9(s_5, s_6, s_7, s_8, s_1, s_2, s_9, s_3, s_4)\Gamma(s_6, s_1) \\
&+ \frac{1-P}{4} \sum_{s_x,s_5,s_6,s_7,s_8,s_9} p_9(s_1, s_2, s_5, s_3, s_x, s_6, s_7, s_8, s_9)\delta(s_2, s_4)\Gamma(s_2, s_x) \\
&+ \frac{1-P}{4} \sum_{s_x,s_5,s_6,s_7,s_8,s_9} p_9(s_5, s_1, s_2, s_6, s_x, s_4, s_7, s_8, s_9)\delta(s_1, s_3)\Gamma(s_1, s_x) \\
&+ \frac{1-P}{4} \sum_{s_x,s_5,s_6,s_7,s_8,s_9} p_9(s_5, s_6, s_7, s_1, s_x, s_8, s_3, s_4, s_9)\delta(s_6, s_2)\Gamma(s_6, s_x) \\
&+ \frac{1-P}{4} \sum_{s_x,s_5,s_6,s_7,s_8,s_9} p_9(s_5, s_6, s_7, s_8, s_x, s_2, s_9, s_3, s_4)\delta(s_6, s_1)\Gamma(s_6, s_x) + \cdots
\end{aligned}
\tag{3}
$$

where $\delta(s_x, s_y)$ denotes the Kronecker delta and the constraint of invasion is expressed as

$$
\Gamma(s_x, s_y) = \begin{cases} 1 & \text{if} \quad s_y - 1 = s_x \bmod 3 \\ 0 & \text{otherwise.} \end{cases} \tag{4}
$$

The terms proportional to P describe the contributions coming from the invasions from an arbitrary distance while the contributions from one of the four nearest-neighbour sites are proportional to $(1 - P)/4$. Equation (3) involves explicitly only those terms coming from the downward invasions. The derivation of the missing terms is straightforward.

At the level of six-site approximation the probability of a nine-site configuration (as shown in figure 6) is expressed by the product of configuration probabilities on 3×2 clusters as

$$
p_9(s_1, \ldots, s_9) = \frac{p_6(s_1, s_2, s_3, s_4, s_5, s_6)\, p_6(s_4, s_5, s_6, s_7, s_8, s_9)}{p_3(s_4, s_5, s_6)} \tag{5}
$$

where the $p_3(s_1, s_2, s_3)$ indicates the configuration probabilities on a 3×1 cluster. Evidently, in this case the invasion of the central site will influence some other six-site configuration probabilities that we can handle in a similar way.

In both cases the corresponding master equations are solved by numerical integration and the results are summarized in figure 5. In agreement with the expectation, the dynamical cluster techniques (at such a high level) reproduce qualitatively well the results obtained by MC simulations. Namely, both descriptions confirm the stability of the central stationary state, that is the area A tends to zero, if $P < P_1^{(4p)} = P_1^{(6p)} = 0.011(1)$. Above this transition point the present approaches predict the appearance of a limit cycle within the range $P_1 < P < P_2$. The area A increases linearly with $P - P_1^{(4p)}$ in the close vicinity of the transition point. Similarly, A approaches 1 linearly for both the four- and six-site approximations, although these methods predict different transition points, i.e., $P_2^{(4p)} = 0.097(3)$ and $P_2^{(6p)} = 0.109(3)$.

These sophisticated techniques have significantly improved the description, and the deviations from the MC results reflect the relevant role of topological features.

5. Conclusions

In summary, cyclic invasions such as the rock-scissors-paper in the three-state systems can maintain a rich variety of spatiotemporal patterns that depend on the quenched and annealed randomness of the background. According to the MC simulations a self-organizing pattern occurs on the square lattice. The classical mean-field and pair approximations are not capable of reproducing this behaviour. It is demonstrated, however, that the extended versions of this approach, called the dynamical cluster technique at the level of four- and six-site approximations, can describe the appearance of this self-organizing pattern.

The quenched randomness is generated by a modified rewiring technique that conserves the degree at each site. For weak quenched randomness the above spatiotemporal pattern remains stable. When the measure of quenched randomness exceeds a threshold value this system undergoes a transition from the symmetric stationary state (central fixed point) to a synchronized oscillation (limit cycle). For annealed randomness this model exhibits similar behaviour with a higher sensitivity to the variation of annealed randomness and above a second threshold value the increasing oscillation terminates at one of the homogeneous (absorbing) states. These features are reproduced qualitatively well by the dynamical cluster technique considering the configuration probabilities on four- and six-site clusters. We think that further systematic analyses can clarify how the transitions are affected on those systems where the quenched randomness and annealed randomness occur simultaneously. More significant modifications of this technique are required if we wish to study the cyclic invasions on networks with arbitrary degree distributions.

Acknowledgment

This work was supported by the Hungarian National Research Fund under grant nos T-33098, F-30499 and Bolyai grant no BO/0067/00.

References

[1] Küpper G and Lortz D 1969 *J. Fluid Mech.* **35** 609
[2] Busse F H and Heikes K E 1980 *Science* **208** 173
[3] Toral R, San Miguel M and Gallego R 2000 *Physica* A **280** 315
[4] Gallego R, Walgreaf M, San Miguel M and Toral R 2001 *Phys. Rev.* E **64** 056218
[5] May R and Leonard W J 1975 *SIAM J. Appl. Math.* **29** 243
[6] Buss L W and Jackson J B C 1979 *Am. Nat.* **15** 223
[7] Tainaka K and Itoh Y 1991 *Europhys. Lett.* **15** 399
[8] Sinervo B and Lively C M 1996 *Nature* **380** 240
[9] Kerr B, Riley M A, Feldman M W and Bohannan B J 2002 *Nature* **418** 171
[10] Nakamaru M and Iwasa Y 2000 *Theor. Popul. Biol.* **57** 131
[11] Szabó G and Czárán T 2001 *Phys. Rev.* E **63** 061904
[12] Czárán T, Hoekstra R F and Pagie L 2002 *Proc. Natl Acad. Sci. USA* **99** 786
[13] Szabó G, Antal T, Szabó P and Droz M 2000 *Phys. Rev.* E **62** 1095
[14] Hauert C, De Monte S, Hofbauer J and Sigmund K 2002 *Science* **296** 1129
[15] Szabó G and Hauert C 2002 *Phys. Rev. Lett.* **89** 118101
[16] Solé R V, Valls J and Bascompte J 1992 *Phys. Lett.* A **166** 123
[17] Tainaka K 1994 *Phys. Rev.* E **50** 3401
[18] Szabó G and Szolnoki A 2002 *Phys. Rev.* E **65** 036115

[19] Hempel H and Schimansky-Geier L 1999 *Phys. Rev. Lett.* **82** 3713
[20] Boerlijst M C and Hogeweg P 1991 *Physica* D **48** 17
[21] Szabó G and Czárán T 2001 *Phys. Rev.* E **64** 042902
[22] Tainaka K 1993 *Phys. Lett.* A **176** 303
[23] Frean M and Abraham E D 2001 *Proc. R. Soc. Lond.* B **268** 1
[24] Szabó G and Hauert C 2002 *Phys. Rev.* E **66** 062903
[25] Kuperman M and Abramson G 2001 *Phys. Rev. Lett.* **86** 2909
[26] Zanette D H 2001 *Phys. Rev.* E **64** 050901
[27] Zanette D H 2001 *Phys. Rev.* E **65** 041908
[28] Watts D J and Strogatz S H 1998 *Nature* **393** 440
[29] Marro J and Dickman R 1999 *Nonequilibrium Phase Transitions in Lattice Models* (Cambridge: Cambridge University Press)
[30] Dickman R 2001 *Phys. Rev.* E **64** 016124
[31] Frachebourg L and Krapivsky P L 1998 *J. Phys. A: Math. Gen.* **31** L287
[32] Zimmermann M G, Equíluz V and San Miguel M 2001 *Economics and Heterogeneous Interacting Agents* ed J B Zimmermann and A Kirman (Berlin: Springer) p 73
[33] Abramson G and Kuperman M 2001 *Phys. Rev.* E **63** 030901
[34] Ebel H and Bornholdt S 2002 *Phys. Rev.* E **66** 056118
[35] Bollobás B 1995 *Random Graphs* (New York: Academic)
[36] Szabó G 2000 *Phys. Rev.* E **62** 7474
[37] Amaral L A N, Scala A, Barthélémy M and Stanley H E 2000 *Proc. Natl Acad. Sci. USA* **97** 11149
[38] Albert R and Barabási A L 2002 *Rev. Mod. Phys.* **74** 47
[39] Dorogovtsev S N and Mendes J F F 2003 *Evolution of Networks* (Oxford: Oxford University Press)
[40] Newman M E J 2003 *SIAM Rev.* **45** 167
[41] Szabó G, Santos M A and Mendes J F F 1999 *Phys. Rev.* E **62** 1095
[42] Hofbauer J and Sigmund K 1998 *Evolutionary Games and Population Dynamics* (Cambridge: Cambridge University Press)